Bio-stimulated synthesis of Zinc oxide Nanoparticles from Andrographis echioides (L.) Nees., characterization and its anti diabetic activity

Uma Maheswari Devi. Palempalli

umadevi66@gmail.com

Sri Padmavati Mahila Visvavidyalayam (Women's University

Niveditha Draksha

Sri Padmavati Mahila Visvavidyalayam (Women's University

Vani Mathakala

Sri Padmavati Mahila Visvavidyalayam (Women's University

Suredsh kumar chitta

Sri krishnadevaraya University

Research Article

Keywords: Zinc oxide Nanoparticles (ZnONps), zeta potential, Andrographis echioides, AFM analysis

Posted Date: December 11th, 2023

DOI: https://doi.org/10.21203/rs.3.rs-3706679/v1

Additional Declarations: No competing interests reported.

Abstract

Green synthesis is based on plant compounds' ability to reduce metal ions and stabilise them into nanoparticles, and it is gaining a lot of attention in recent years. It has been shown to be a reliable and alternate method for the development of novel Nanoparticles*. Andrographis echioides (L.) Nees* is a used to synthesize zinc oxide nanoparticles*.* UV-visible spectroscopy, FTIR, Zeta potential, particle size analysis, XRD, SEM, AFM analysis were adopted to characterise the capped ZnONPs. The intense surface Plasmon resonance bands of ZnONPs at 340 nm confirmed the green synthesis of ZnONPs. The various functional groups of *A.echioides*involved in the synthesis and crystalline nature of ZnO Nanoparticles were identified using FTIR and X-ray diffraction respectively. The average particle size was found to be 4.0 nm, and the zeta potential value was -11 mV. Administration of ZnONPs significantly reduced the blood glucose level and HbA1C when compared with standard drug glibenclamide in STZ- induced in-vivo models. The antidiabetic potential of ZnONPs was confirmed by numerous biochemical parameters like serum lipid profiles, liver and renal functional markers and regeneration β- cells of islets of Langerhans in STZ- induced diabetic rats. Thus, the ZnONPs synthesized from *A. echioides*were found to be effective anti-hyperglycemic agent in the management of diabetes.

Introduction

Nanomaterials have a wide range of properties when scaled down from bulk size to nanometre size, which has enabled their application in a several fields (Devasenan et al., 2016). Nanoparticles (NPs) play an essential role in the surface area to volume ratio, and this leads them to become more reactive. Synthesis of NPs includes three different methods namely physical, chemical and biological (Anantharaman et al., 2020). Among which physical and chemical procedures are simpler and easier, but their utility is limited due to the usage of harmful substances (supraja et al., 2015) Green synthesis of nanoparticles utilising plant and their extracts is an alternative, affordable method and also environment friendly (Yugandhar et al. 2018). Metal ions are reduced to nanoparticles in a single step by phytochemical constituents of plant extracts. At room temperature and pressure, this biogenic conversion of a metal ion to a base metal occurs rapidly and is easily scaled up. (Sadeghi et al., 2014)

Among the metallic nanoparticles, Zinc oxide (ZnO) NPs is of maximum interest because they are inexpensive to produce, safe and can be prepared easily (Happy Agarwal et al., 2017). It is well-known that all tissues in the body, including the brain, muscle, bone, and skin, contain significant amount of zinc, an essential trace element. Zinc participates in the body's metabolism and a vital component in several enzyme systems, and also involved in the synthesis of proteins and nucleic acids, hematopoiesis, and neurogenesis (Jinhuan Jiang et al., 2018). Zinc is the key element that keeps insulin's structure and functionality intact. The zinc transporter ZnT8 is known to have a significant and active part in the manufacture of insulin in beta-cells, which contain high quantities of zinc about 70% in the insulin secretory granules (Nicolson et al., 2009). Numerous researchers explored the association between zinc levels and issues pertaining to diabetes mellitus. Scientists have conducted research on zinc-related medications for the treatment of diabetes owing to the role of zinc in pancreatic function and diabetes

but the oral zinc supplementation does not result in the management of pertaining diabetes (Scott and Fisher 1938). This totally shifted the focus of the research to other strategies for supplementing zinc, with nanotechnology currently providing the best opportunities (Venkata kotakadi et al., 2021). Small particle size nano-ZnO makes zinc easier for the body to absorb. Nano-ZnO is therefore frequently used as a food ingredient. ZnONPs have generated increased interest in biomedical applications, and the US FDA has designated ZnO as a GRAS (generally recognised as safe) metal oxide (Jinhuan Jiang et al., 2018). According to Umrani and Paknikar (2014), the first treatment for diabetes based on zinc oxide nanoparticles has been developed. The findings of the study were beneficial, and zinc oxide nanoparticles (ZnONPs) showed to be safe even at greater concentrations.

Thus, the present report focused on the synthesis of ZnONPs using extract of *Andrographis echioides (A.echioides).* More than 20 species of *Andrographis* (Acanthaceae) have been reported to occur in India. *Andrographis echioides* (L) Nees, also known as *Indoneesiella echioides* (L) Nees (Acanthaceae), an annual herb plant is used to treat goiter (Elaiyaraja et al., 2016), liver diseases, fever, fertility problems, bacterial (Qadrie ZL et al., 2009) malarial, helmintic, fungal, diarrhoea and larvicidal disorders (Nazar S et al., 2009).

Basically, the current work presents a green, quick, affordable, and reliable strategic method to synthesise ZnONPs utilising *A.echioides* and to investigate the anti-hyperglycemic activity of ZnONPs by activating the regeneration of β -cells of islets of Langerhans to produce more insulin (Antony Samy Agnel Ruba et al., 2016). However, there is no literature on green synthesis of ZnONPs from *A.echioides* and validation of invivo antidiabetic activity. Hence, the present work has been undertaken to synthesize ZnONPs and evaluating the antidiabetic activity of *Ae*-ZnONPs and on comparision with an ethanolic extract of the *A.echioides* leaves using STZ-induced diabetic rats.

Materials and Methods

Preparation of A.echioides leaf extract

The leaves of *A.echioides* (L.) Nees (*A.e*), collected from the Tirumala hills, were sliced into small pieces, cleaned, shade-dried, and pulverised in a Wiley mill. (Fig. 1) The leaf powder(10 gms) was then mixed with 100 ml of Milli Q water and boiled for about 20 minutes. The mixture was then cooled to room temperature and filtered. The filtrate was then used as an aqueous leaf extract for the biosynthesis of *Ae*-ZnONPs. Further 10 gms of leaf powder was mixed with 100 ml of ethanol and was extracted using Soxhlet apparatus. Then the solvent was completely evaporated at 60º c using a Rotary evaporator and later *A.echioides* ethanolic extract (AeEE) was collected and used for further analysis.

Green synthesis of Zinc oxide nanoparticles

An aliquot of 10 ml of aqueous extract was combined with 50 ml of 0.1M Zinc acetate and the homogenous mixture was kept on magnetic stirrer for 4hours at room temperature until the formation of white coloured precipitate. The pH of the mixture was maintained at 12 by adding 1.0 M NaOH. The

precipitate was centrifuged at 10,000 RPM for 10 min to separate agglomerated, broad sized particles. After centrifugation, the pellet was collected and dried at 80^0c for 8 hours. The dried pellet comprising the ZnONPs, was powdered and designated as *A.echioides* Zincoxide Nanoparticles *(Ae*-ZnONPs). The powdered *Ae*-ZnONPs were stored in sterile vials for further characterization by UV-VIS, FTIR, Particle size analysis, Zeta potential, XRD, SEM, AFM analysis.

Characterization of bioinspired Ae -ZnONPs

The formation of NPs at the initial stage is confirmed by UV- visible spectroscopic analysis. About 1 mg powder of *Ae*-ZnONPs was dissolved in sterile water and the λ max of *Ae*-ZnONPs was recorded in the range of 200–400 nm using UV-1601, SHIMADZU spectrophotometer. The size and distribution of the *Ae*-ZnONPs synthesised nanoparticles was analysed based on the dynamic light scattering and zeta potential.(Nanopartica analyser, Horiba SZ 100, Japan) FTIR spectral analysis was carried out to spot the functional groups of plant metabolites involved in the reductive synthesis and capping of *Ae*-ZnONPs. The spectra of *Ae*-ZnONPs were recorded in between 400–4000 cm^{-} in mid region of FTIR spectrophotometer (Alpha BRUKER, Switzerland).Using the X-ray diffraction technique, the phyto-reduced *Ae* -ZnONPs were characterised to reveal their crystal structure by comparing with JCPDS. The XRD pattern was obtained at 40 kV and 20 A using a computer-controlled XRD device (Shimadzu, XRD-6000). Micro structural images of biosynthesized *Ae*-ZnONPs were captured using a Nova NanoSEM 450 analyzer with an acceleration voltage of 10 KV. The elemental details of *Ae*-ZnONPs and its composition were obtained using energy dispersive spectroscopy. The Atomic Force Microscopy (AFM) was used to disclose the topology and morphological features of *Ae*-ZnONPs. The AFM samples were prepared by dropping the *Ae*-ZnONPs solution onto the glass slide through hanging drop method. The slide was allowed to dry at room temperature and AFM analysis was performed. (NX10-AFM park systems)

In vivo antidiabetic activity of Ae-ZnONPs

Experimental Animals

Adult healthy male wistar rats of the age group 8–12 weeks weighing 150-240g were acclimatized and maintained at standard condition for the experimental analysis as per the guidelines of Institutional Animal Ethical Committee No. CPCSEA/1677/PO/Re/s/2012/IAEC/03.

Induction of diabetes in Wistar Rats

STZ induced diabetic rats were used as in-vivo models for experimental analysis (Williamson et al., 1969). In concise, a streptozotocin (STZ 50 mg/kg bwt) dispersed in cold freshly prepared 0.01M citrate buffer pH 4.5, was injected intraperitoneally to rats in fasting for 12 h. To manage the drug-induced hypoglycemia, a 5% sugar solution was given to the animals. Following 72 hours of injection, blood was collected from overnight fasting rats and blood glucose concentration was determined by a glucometer. The rats with fasting blood glucose concentrations greater than 200 mg/dl or 15 mM/l were marked and utilized as *in vivo* diabetic models for further experimental analysis. Control animals were given normal

saline alone (kotha et al., 2017). The diabetic rats were independently treated daily with glibenclamide, ethanolic extract and *Ae*-ZnONPs orally in aqueous solution for 40 days.

Experimental Design for long term Treatment

The 36 experimental animals were categorized into six experimental groups namely, Rats received normal saline (NC), Rats treated with 10 mg *Ae*-ZnONP /kg b.w/day (NT), Rats induced with STZ 50mg/kg b.wt (DC), Diabetic rats treated with 20 mg of glibenclamide/ kg b.w/day (DG), Diabetic rats treated with 500 mg AeEE/kg b.w/day (DT), Diabetic rats treated with 10 mg *Ae*-ZnONP/kg b.w/day (DNP).

The body weight of experimental rats treated with AeEE and Ae-ZnONP was assessed in comparison with control rats at regular intervals i.e. 7, 14, 21, 28, 35 and 40th day of experiment

Effect of Ae-ZnONPs on biochemical parameters of Experimental rats

Blood was drawn from tip of the tail vein of experimental rats and Fasting blood glucose levels were assessed by Glucose oxidase-peroxidase method using single touch glucometer (Vani et.al., 2020). The results were reported in terms of milligram per deciliter of blood. HbA1C was determined as per the method of Eross et al., 1984 and the values were expressed as percentage of glycosylated haemoglobin. The quantity of serum cholesterol was calculated according to the method of Zlatkis et al. 1953. Foster and bunn (1973) method was used to estimate serum triglycerides. According to Friedewald, Levy, and Fredrickson (1972), Serum HDL-cholestrol, VLDL and LDL were estimated as per the standard methods. Plasma SGOT and SGPT enzyme levels were measured by Reitman and Frankel method (Reitman and Frankel 1957). The serum alkaline phosphatase (ALP) was estimated by p-nitro phenyl phosphate method (Bessey, Lowry, and Brock 1946). Serum creatinine & Serum urea concentrations were determined by Jaffe's and diacetyl monoxime methods respectively (Slot 1965; Wybenga, Giorgio, and Pileggi 1971).

Histopathology of tissues

After 40 days of experimental period, the rats from all the six groups were sacrificed by cervical dislocation using minimal anesthesia and dissected. The liver, kidney, pancreas were collected and rinsed three times using saline and stored in 10% formalin solution for histopathological analysis. The tissues were processed into thin 5 µm sections using a rotator microtome, dehydrated and embedded in paraffin blocks. Later deparaffinized sections were treated with hematoxylin for 10 min, followed by rinsing with water, 1% acid alcohol, 1% lithium carbonate. Further the slides were counter stained with eosin, washed and mounted on glass slides for observation under 4X and 10X magnification.

Statistical analysis

A group of 6 animals was used for each set of experiments and values represented are mean ± S.D(standard deviation) calculated utilising Graph pad prism version 7.0. The findings were evaluated

using One-Way ANOVA and Statistical significance is indicated by an asterisk (*) where *p* values are *$p < 0.05$, **$p < 0.01$ and ***$p < 0.001$.

Results and Discussion

Andrographis echioides, a dry land annual herb of southern India is widely recognized species of genus Andrographis (Mativanan and Suseem,2015). *A.echioides* is listed in the Indian Materia Medica (Savilikadi et al 2020) due to its potential application in the treatment of dysentery, cholera, Jaundice. The diversified phytochemicals of *A.echioides* are contributing to several therapeutic applications such as antimicrobial, anti-oxidant, antidiabetic, antipyretic, anti-inflammatory activities. Due to the remarkable biological activities and wide spread abundance, *A.echioides* is being expoilted at a rapid rate. Thus, the leaf extract of *A.echioides* was utilized for the bioinspired green synthesis of ZnONPs.Initially, the phytomediated synthesis of ZnONPs by using *A.echioides* was confirmed with the visual characterization of colour change pattern from green to pale white colour. (Fig. 2)

UV-Vis Spectral analysis

The colour change clearly indicates the bioreduction of zinc salts into ZnONPs by the bioactive constituents of *A.echioides.* The bioreduction of zinc was found to be extracellular and indicates the significance of phyto approach in the synthesis of metallic nanoparticles.

The reduction and stability of *Ae*-ZnONPs was analysed by UV-Vis Spectral analysis. *Ae*-ZnONPs exhibited a significant shift in the excitonic absorption from 262 nm of *A.echioides* aqueous extract to 340 nm. (Fig. 3a) As per the literature, the λ max of ZnO nanoparticles varies from 310 to 360 nm which totally relays on surface plasmon resonance and the calcination process (Satyanarayana et al., 2012). The band gap energy was calculated as 3.6 ev using E = 1240/340 absorbance which is intune with reported energy values of ZnO nanoparticles (Jayachandran et al., 2021).

(b) FTIR spectra representing the Molecular signatures of functional groups in AeAE and phytogroups involved in the synthesis of *Ae*-ZnONPs

Fourier Transform Infrared spectroscopy

The reductive synthesis, capping and stabilization of *Ae*-ZnONPs nanoparticles by different phytochemical constituents of *A.echioides* was detected through FTIR spectral analysis. *Ae*-ZnONPs shows strong broad peak at 3326 cm^{-1} correlates to O-H bond of alcohol and phenol. An absorption peaks at 1565.18 cm^{-1} and 1439.04 cm − 1 indicates N-H bending of amine and O-H bending of alcohol respectively, 1021.85cm^{-1} corresponds to (C–N) amine stretching, 479.01 cm^{-1} corresponds to poly sulfides stretch (S-S), 421.53 cm^{-1} was attributed to the Zn-O extending vibration (Fig. 3b). The molecular signatures at 3453 cm^{-1}, 1632 cm^{-1} corresponds to phenols and alkenes of *A.echioides* leaf extract which facilitated the capping and stabilization of ZnONPs. Narayanan et al., (2023) reported the

presence of OH and ZnO functional groups in ZnO nanocomposites and their spectra between 600 and 400 cm^{-1}.

Dynamic light scattering of Ae-ZnONPs

The average diameter and particle size distribution of biosynthesized *Ae*-ZnONPs were calculated based on dynamic light scattering resulting from the Brownian motion of the nanoparticles. Zeta potential, which calculates the attraction or repulsion impact raised by fluctuations in charge densities, is used to evaluate the stability of synthesised nanoparticles. *Ae*-ZnONPs shows particle size of 4.0 nm (Fig. 4a) and zeta potential of -11mV, (Fig. 4b) both of which indicates the presence of repelling electro-static forces among the synthesized zinc nanoparticles, which causes the particle to mono disperse. If the hydrosols have a strong negative or positive zeta potential then they will tend to reject one another and the particles will not have tendency to aggregate. This indicates synthesized nanoparticles have higher stability in a liquid medium. Similar findings were obtained in the green synthesis of zinc oxide nanoparticles from leaf extract of *Andrographis serpilifolia.* (Venkata S.kotakadi et al. 2021)

x-ray Diffraction analysis of Ae-ZnONPs

The crystalline structure and the nano size of *Ae*-ZnONPs was detected with XRD. As shown in the Fig. 5, nanoparticles were polycrystalline in nature, showing multiple diffraction peaks at 34.50°, 36.27°, 47.78°, 56.77°, 63.54°, 66.54°, 68.70°, 72.58° and 77.16° were corresponding to planes of (002), (101), (102), (110), (103), (200), (112), (004), and (202). The planes represent the wurtzite's hexagonal crystal structure. All of the observed planes were matched well with the JCPDS card number: 75–0576. These results were consistent with EDAX analysis. The wurtzite crystal structure of *Ae*-ZnONPs is in agreement with the XRD diffraction profile of ZnONPs synthesized using vegetable extracts (Anatol Degefa et al., 2021)

Atomic force microscopy (AFM)

Atomic force microscopy is one of the most effective imaging technique for determinig size, morphology and distribution of synthesized nanoparticles. The- 2D and 3D images displayed spherical and Poly-dispersed and non-agglomerated multi-fold shaped particles with sizes ranging from 20 to 78 nm (Fig. 6). Similar type of AFM results were reported on synthesis of ZnONPs utilising Albizia aman (Jacq.) Merr. leaf extract. (Azharuddin Daphedar et al., 2018).

(a) 5 µm resolution **(b)** 3dimensional view of *Ae*-ZnONPs

Scanning Electron Microscopy (SEM) and Energy dispersive x-ray (EDX)analysis

SEM images were captured to determine the shape and size of the synthesized nanoparticles, as shown in Fig. 7a. The synthesis of nanoparticles is confirmed by the surface morphology of nanoparticles and that were found to be mostly spherical in shape, poly dispersed in condition and grain size ranging from

80–120 nm. The spherical shaped nanoparticles was reported in *Andrographis paniculata* extract mediated ZnONPs (Devasenan et al., 2016). The EDX analysis detects the elements in the synthesized nanoparticles. As depicted in the Fig. 7b, ZnONPs revealed that weight percentage of zinc and oxide in the sample were 36.22 and 32.45. These outcomes suggested that the reduced nanoparticles are zincoxide and weak peak of sodium, Potassium, calcium might have originated from X-ray emission of carbohydrates/proteins/enzymes present on the surface of *Ae*-ZnONPs from the leaf extract of *Andrographis echioides*. High concentration of zinc and oxide in the synthesized ZnONPs show the purity of the compound. Similar type of outcomes were observed on the green synthesis of. ZnONPs using Aeromonas hydrophila. (Jayaseelan et al., 2012)

(b) EDX analysis of synthesized *Ae*-ZnONPs

Effect on body weight

The impact of AeEE and *Ae*-ZnONPs on total body weight of normal and diabetic experimental animals illustrates in Fig. 8. Normal rats were observed to be constant in their body weight but diabetic rats exhibited significant decline in body weight over 40 days. STZ causes weight loss which was significantly ($P < 0.01$) recovered with the treatment. Diabetic rats treated with the AeEE, *Ae*-ZnONP and glibenclamide revealed significant rise in body weight when compared to the STZ control animals, thus exhibiting considerable benefit in preventing the loss of body weight in diabetic rats. *Ae*-ZnONPs (10 mg/kg b.w) at a 50–fold lower concentration to AeEE (500 mg/kg b.w) exhibited equivalent impact in regaining the body weight. It confirms the impact of *Ae*-ZnONPs in the management of diabetes without any side effects

Rats received normal saline (NC), : Rats treated with 10 mg *Ae*-ZnONP /kg b.w/day in solution orally for 40 days (NT), Rats induced with STZ 50mg/kg b.wt in citrate buffer (DC), Diabetic rats treated with 20 mg of glibenclamide/ kg b.w/day in aqueous solution for 40 days (DG), Diabetic rats treated with 500 mg AeEE/kg b.w/day in aqueous solution orally for 40 days (DT), Diabetic rats treated with 10 mg *Ae*-ZnONP/kg b.w/day in aqueous solution orally for 40 days (DNP). Results are presented as mean ± S.D of six rats from each group, statistical significance ($p \leq 0.05$)

Invivo Antidiabetic activity of A.echioides ethanolic extract & Ae-ZnONps

Effect on Fasting Blood Glucose and HbA1c levels

The glucose levels significantly ($p < 0.05$) increased in STZ induced diabetic rats than control rats (Fig. 9). Diabetic rats treated with oral supplementation of AeEE, *Ae*-ZnONps and glibenclamide had significant reduction in the glucose and HbA_1c levels which are equivalent to normal range. In both diabetic and control rats, the levels of glucose and HbA1c were unchanged. *Ae*-ZnONPs proved to be strong in exhibiting antihyperglycemic action at a considerably lower dose (10 mg/kg b.w) than AeEE (500 mg/kg b.w). Moreover, it has been reported that zinc control glucagon release from pancreatic α-cells. Therefore, glucagon-stimulated hepatic pathways (i.e., gluconeogenesis, glycogenesis) would be

obstructed in the fasting state of mice which may result in decreased blood glucose concentrations following zinc supplementation. (Siddiqui SA et al., 2020)

Effect on serum lipid profile

As demonstrated in Fig. 10a total cholesterol, triglycerides, LDL, and VLDL cholesterol were significantly elevated and HDL cholesterol values were significantly reduced in STZ- induced diabetic rats as compared to normal control rats. This is mostly due to lower insulin levels and these adverse effects could be caused by hormones that promote cholesterol production and/or reduce lipolysis. Conversely, Serum lipid profiles in diabetic rats treated with AeEE, *Ae*-ZnONPs, or glibenclamide significantly reduced, whereas HDL cholesterol elevated. The results showed that *Ae*-ZnONPs (10 mg/kg b.w) treated rats exhibits better lipid profile when compared to the AeEE (500 mg/kg b.w) treated rats. Similar findings from earlier research indicate that Zinc (Zn) is crucial in the organisation of metalloenzymes involved in the digestion and absorption of lipids. The improved lipid profile levels following treatment with *Ae*-ZnONPs may be related to Zn's crucial function in enzymatic reactions since Zn can act as α - blocker, as shown in the treatment of dyslipidemia (Zahraa Alaaeldein Gadoa et al., 2022)

Effect on the liver marker enzymes and kidney function markers

Liver marker enzymes such as SGOT, SGPT & ALP significantly elevated in diabetic control rats (Fig. 10b). Similarly, renal functional markers Urea and Creatinine were significantly elevated in diabetic rats as compared to normal control rats (Fig. 10c, 10d). After oral treatment with AeEE, *Ae*-ZnONPs, independently drastic reduction in the liver functional markers was noticed in diabetic rats. When compared to diabetic control rats, diabetic rats administered with glibenclamide observed significantly lower levels of liver marker enzymes. The similar trend of reduced levels of renal functional markers was exhibited in experimental diabetic rats treated with AeEE, *Ae*-ZnONPs and glibenclamide. The impact was found to be significant (liver enzymes, urea and creatinine) with *Ae*-ZnONPs at a very low concentration when compared with glibenclamide and AeEE. *Ae*-ZnONPs improves serum insulin levels by elevating the insulin gene mRNA expression. Here, ZnO nanoparticles may contribute to improved glucose uptake and metabolism by regulating the development of hepatic glycogenesis (Alkaladi et al.,2014). The fact that zinc has a direct role in the total metabolism of carbohydrates, proteins, and lipids confirms the significance of *Ae*-ZnONPs in demonstrating antidiabetic activity. zinc is a cofactor of the important enzymes involved in glucose metabolism. (Hassan et al. 2021)

Effect of AeEE, Ae-ZnONPs on histopathology characterization of pancreas

The pancreatic tissues from control animals revealed normal islets of Langerhans acini and cells (Fig. 11). In contrast, in diabetic rats, the pancreas cells deteriorated with multiple foci of haemorrhage, necrosis, and tubules edema. No histological changes were exhibited in pancreas of both control and diabetic rats. When compared to diabetic rats, rats treated with AeEE, *Ae*-ZnONPs show a regenerative

effect on the typical cellular size of islets of pancreatic tissue and remarkable change was noticed with very low concentrations of *Ae*-ZnONPs. This confirms the potential application of *Ae*-ZnONPs in the management of diabetes through anti-hyperglycemic activity. Numerous studies show that zinc is released with insulin and act as an autocrine molecule to increase the release of insulin in response to glucose in the pancreatic islets of isolated rats. ZnO nanoparticles can serve as an insulin secretagogue due to the stimulation of another physiological mechanism such as insulin release, glucagon regulation and glucose accumulation in the liver and adipose tissue. Zinc transporters are identified in adipose tissues and liver as these tissues are important in glucose metabolism regulation (Siddiqui SA et al., 2020). Intake of Zinc can enhance clinical outcomes associated with glycaemia in diabetes. (J. Rungby et al., 2010)

Conclusion

The present investigation focused on biosynthesis of ZnONPs using *A.echioides* extract and their antidiabetic activity.The administration of *Ae*-ZnONPs to STZ-induced hyperglycemic male wistar rats showed antidiabetic effects highlighting the potential efficiency of synthesised ZnONPs. Therefore, it was suggested that *Ae*-ZnONPs can contribute to effective intracellular drug distribution because it is readily absorbed by negatively charged cellular membranes. Further implications include that *A. echioides* will serve as a promising target in alternative treatments for the efficient treatment of diabetes and especially *Ae*-ZnONPs may be an evoking medicine for treating Type-2 diabetes.

Declarations

Conflict of interest statement

On behalf of all authors, the corresponding author declares that there is no conflict of interest.

Author Contribution

all authors are contributed equally

Acknowledgements

We thank DST-CURIE laboratory, IPT, SPMVV for providing us the instrumental facility required for the study.

References

1. Alkaladi A. Aaser Mohamed Abdelazim and Mohamed Afifi. Antidiabetic Activity of Zinc Oxide and Silver Nanoparticles on Streptozotocin-Induced Diabetic Rats. Int J Mol Sci *15*. 10.3390/ijms15022015.
2. Anantharaman S, Rego R, Muthakka M, Anties T, Honnur K. (2020) *Andrographis paniculata*-mediated synthesis of silver nanoparticles: antimicrobial properties and computational studies. SN Appl. Sci. 2014; 2, 1618. https://doi.org/10.10007/s42452-020-03394-7.
3. Anatol D, Bulcha B, Jule LT, Fikadu B, Ramaswamy S, Lalitha Priyanka D, Nagaprasad N, Krishnaraj R. Green Synthesis, Characterization of Zinc Oxide Nanoparticles, and Examination of Properties for Dye-Sensitive Solar Cells Using Various Vegetable Extracts. J Nanomater. 2021;3941923:9. https://doi.org/10.1155/2021/3941923.
4. Ruba ASA. Asirvatham Doss, Veerabahu Ramasamy Mohan. Evaluation of *in vivo* antidiabetic activity of *Andrographis echioides* (l.) nees. Int. Res. J. Pharm. 2016; 7 (6) WSN 55 38–50 EISSN 2392 – 2192.
5. Ashwini Jayachandran, Aswathy TR, Achuthsankar S, Nair. (2021) Green synthesis and characterization of zinc oxide nanoparticles using Cayratia pedata leaf extract. j.b b rep 2021; https://doi.org/10.1016/j.bbrep.2021.100995.
6. Azharuddin D, Taranath TC. Green synthesis of zinc nanoparticles using leaf extract of *Albizia saman* (Jacq.) Merr. and their effect on root meristems of *Drimia indica* (Roxb.) Jessop, Caryologia. 2018; 71:2, 93–102. 10.1080/00087114.2018.1437980.
7. Bessey OA, Lowry OH, Brock MJ. A method for the determination of alkaline phosphatase with five cubic millimeters of serum. JBC. 1946;164:321–9. S0021-9258(18)43072-4.
8. Devasenan S, Hajara Beevi N, Jayanthi SS. Green Synthesis and Characterization of Zinc Nanoparticle Using *Andrographis paniculata* Leaf Extract. Int J Pharm Sci Rev. 2016;39(1):48: 243–7.
9. Elaiyaraja A, Chandra mohanG. Isolation and Characterization of 4',7-dihydroxy isoflavone from *Indoneesiella echioides* (L.) Nees plant leaves. WSN. 2016;55:38–50.
10. Eross J, Kreutzmann D, Jimenez M, Keen R, Rogers S, Cowell C, Vines R, Silink M. Colorimetric measurement of glycosylated protein in whole blood, red blood cells, plasma and dried blood. Ann Clin Biochem. 1984;21:477–83. 10.1177/000456328402100606.
11. Foster LB, Dun RT. Standard reagents for determination of serum triglycerides by colorimetric Hantz condensation method. JLab Clin Med. 1973;19:338–40.
12. Friedewald WT, Levy RI, Fredrickson DS. Estimation of the concentration of LDL-cholesterol in plasma without the use of the preparative ultracentrifuge. Clin Chem. 1972;18(6):499–502. 10.1093/clinchem/18.6.499.
13. Gadoa ZA, Moustafa AH, Rayes E, Arisha SM, Mansour AA. MF. Zinc Oxide Nanoparticles and Synthesized Pyrazolopyrimidine Alleviate Diabetic Effects in Rats Induced by Type II Diabetes. ACS Omega. 6;7(41):36865–36872. 10.1021/acsomega.2c05638. PMID: 2022; 36278044; PMCID: PMC9583298.

14. Happy Agarwal, Venkat Kumar S, Rajesh kumar S. A review on green synthesis of zinc oxide nanoparticles – An eco-friendly approach. Resource efficient technologies. 2017;3(4):406–13. https://doi.org/10.1016/j.reffit.2017.03.002.
15. Hassan RM, Elsayed M, Kholief TE, et al. Mitigating effect of single or combined administration of nanoparticles of zinc oxide, chromium oxide, and selenium on genotoxicity and metabolic insult in fructose/streptozotocin diabetic rat model. Environ Sci Pollut Res. 2021;28:48517–34. https://doi.org/10.1007/s11356-021-14089-w.
16. Jayaseelan C, Rahuman AA, Kirthi AV, Marimuthu S, Santhoshkumar T, Bagavan A, et al. Novel microbial route to synthesize ZnO nanoparticles using Aeromonas hydrophila and their activity against pathogenic bacteria and fungi. Spectrochim Acta A Mol Biomol Spectrosc. 2012;90:78–84. 10.1016/j.saa. 2012.01.006.
17. Jinhuan Jiang J, Pi J, Cai. The Advancing of Zinc Oxide Nanoparticles for Biomedical Applications. Hindawi Bioinorg Chem Appl. 2018;1062562. https://doi.org/10.1155/2018/1062562.
18. Kotha P, Badri KR, Nagalapuram R, Allagadda R, Chippada AR. Anti-Diabetic Potential of the Leaves of Anisomeles malabarica in Streptozotocin Induced Diabetic Rats. Cell Physiol Bioc. 2017; hem 43(4):1689–1702. doi: 10.1159/000484030. Epub 2017 Oct 18. PMID: 29045936.
19. Mathivanan D, Suseem SR. Phytochemical and pharmacological review of Andrographis echiodies. J Chem Pharm Res. 2015;7(7):1167–71.
20. Narayanan KB, Bhaskar R, Seok YJ, Han SS. Photocatalytic Degradation, Anticancer and Antibacterial Studies of *Lysinibacillus sphaericus* Biosynthesized Hybrid Metal / Semiconductor Nanocomposites. Microorganisms. 2023;11(7):1810. https://doi.org/10.3390/microorganisms11071810.
21. Nazar S, Ravikumar S, William GP, Syed Ali M, Suganthi P. Screening of Indian coastal plant extracts for larvicidal activity of *Culex quinquefasciatus*. Indian J Sci Technol. 2009;2(3):24–7. 10.17485/ijst/2009/v2i3/29407.
22. Nicolson TJ, Bellomo EA, Wijesekara N, Loder MK, Baldwin JM, Gyulkhandanyan AV, Koshkin V, Tarasov AI, Carzaniga R, Kronenberger K, et al. Insulin storage and glucose homeostasis in mice null for the granule zinc transporter ZnT8 and studies of the type 2 diabetes-associated variants. Diabetes. 2009;58(9):2070–83. 10.2337/db09-0551.
23. Pandarinath S, Phanikanth J, Gulab Khan R, Raghu E, Sandhya D, Venkateswar Rao A, Sadanandam A. Direct regeneration and genetic fidelity analysis of regenerated plants of Andrographis echioides (L.) - An important medicinal plant. Ind Crops Prod. 2020;155:0926–6690. https://doi.org/10.1016/j.indcrop.
24. Yugandhar P, Vasavi T, Jayavardhana Rao Y, Uma Maheswari Devi P, Golla Narasimha SN, Cost, Effective. Green Synthesis of Copper Oxide Nanoparticles Using Fruit Extract of Syzygium alternifolium (Wt.) Walp., Characterization and Evaluation of Antiviral Activity. J Clust Sci 29:743–55. 10.1007/s10876-018-1395-1.

25. Qadrie ZL, Beena Jacob, Anandan R, Rajkapoor B, Rahamathulla M. Antibacterial activity of ethanol extract of *Indoneesiella echioides* evaluated by the filter paper disc method. Pak J Pharm Sci. 2009;22(2):123–5.
26. Reitman S, Frankel S. A colorimetric method for the determination of serum glutamic oxalacetic and glutamic pyruvic transaminases. Am J Clin Pathol. 1957;28(1):56–63. 10.1093/ajcp/28.1.56.
27. Rungby J. Zinc, zinc transporters and diabetes. Diabetologia. 2010;53(8):1549–51. 10.1007s00125-010-1793-x.
28. Sadeghi B, Gholamhoseinpoor F. A study on the stability and green synthesis of silver nanoparticles using Ziziphora tenuior (Zt) extract at room temperature. Spectrochim Acta A Mol Biomol Spectrosc. 2014;134:310–5. 10.1016/j.saa.2014.06.046. Epub 2014 Jun 19. PMID: 25022503.
29. Satyanarayana T, Srinivasa Rao K, Nagarjuna G. Synthesis, characterization and Spectroscopic Properties of ZnO Nanoparticles. Int sch res notices. 2012. https://doi.org/10.5402/2012/372505. 372505,6.
30. Scott DA, Fisher AM. The insulin and the zinc content of normal and diabetic pancreas. J Clin Investig. 1938;17(6):725–8. 10.1172/JCI101000.
31. Siddiqui SA, Or Rashid MM, Uddin MG, Robel FN, Hossain MS, Haque MA, Jakaria M. Biological efficacy of zinc oxide nanoparticles against diabetes: a preliminary study conducted in mice. Biosci Rep 30;40(4):BSR20193972. 10.1042/BSR20193972. PMID:2020; 32207527; PMCID: PMC7138905.
32. Slot C. (1965) Plasma creatinine determination. A new and specific Jaffe's reaction method. Scand *J* Clin *Lab* Invest. 1965;*17*(*4*):*381*–38*7*. 10.3109/ 00365516509077065.
33. Supraja N, Prasad TNVKV, Giridhara Krishna T, David E. Synthesis, characterization, and evaluation of the antimicrobial efficacy of Boswellia ovalifoliolata stem bark-extract-mediated zinc oxide nanoparticles. Appl Nanosci. 2016;6:581–90. 10.1007/s13204-015-0472-0.
34. Umrani RD, Paknikar KM. Zinc oxide nanoparticles show antidiabetic activity in streptozotocin-induced Type 1 and 2 diabetic rats. Nanomed (Lond). 2014;9(1):89–104. 10.2217/nnm.12.205.
35. Vani M, Maheswari Devi U. Seagrass in the Control of Hyperglycemic and Hyperlipidemic States of Streptozotocin Induced Diabetic Rats. Pharmacognos J. 2020;12(6):1716–21. 10.5530/pj.2020.12.232.
36. Venkata SK, Susmila Aparna G, Peddana K, Rajesekhar A, Appa Rao C, Sai Gopal DVR. Bio-inspired multifunctional zinc oxide nanoparticles by leaf extract of *Andrographis serpilifolia* and their enhanced antioxidant, antimicrobial, and antidiabetic activity—a 3-in-1 system. Part Sci Technol. 2022;40(4):485–99. 10.1080/02726351.2021.1966145.
37. Williamson JR, Browning ET, Scholz R. Control mechanisms of gluconeogenesis and ketogenesis. J Biol Chem. 1969;244(17):4607–16.
38. Wybenga DR, Giorgio JD, Pileggi VJ. Manual and automated methods for urea nitrogen measurement in whole serum. Clin Chem. 1961;17(9):891–5. 10.1093/clinchem/17.9.891.
39. Zlatkis A, Zak B, Boyle AJ. A new method for the direct determination of serum cholesterol. J Lab Clin Med. 1953;41(3):486–92. PMID: 13035283.

Figures

Figure 1

Leaves of *Andrographis echioide*s

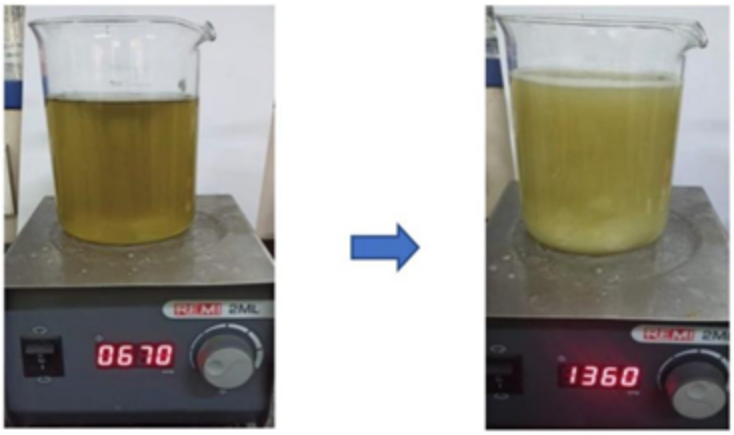

Figure 2

phytomediated synthesis of ZnONPs using aqueous leaf extract of *Andrographis echioides*

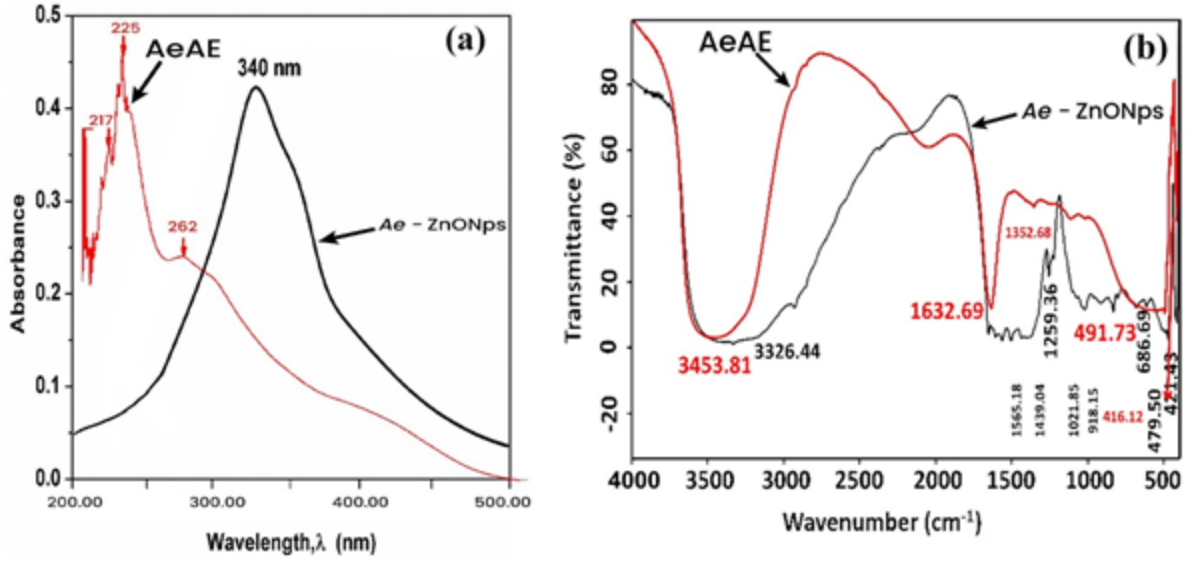

Figure 3

(a) Absorption maxima of AeEE (225 nm) and Ae-ZnONPs (340nm)

(b) FTIR spectra representing the Molecular signatures of functional groups in AeAE and phytogroups involved in the synthesis of *Ae*-ZnONPs

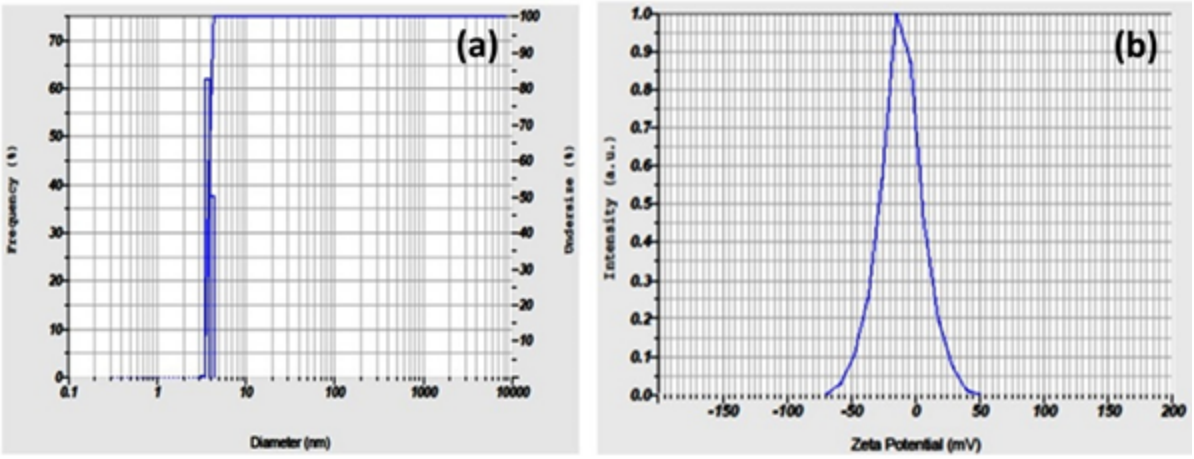

Figure 4

(a) Particle size of *Ae*-ZnONPs **(b)** zeta potential of the synthesized *Ae*-ZnONPs

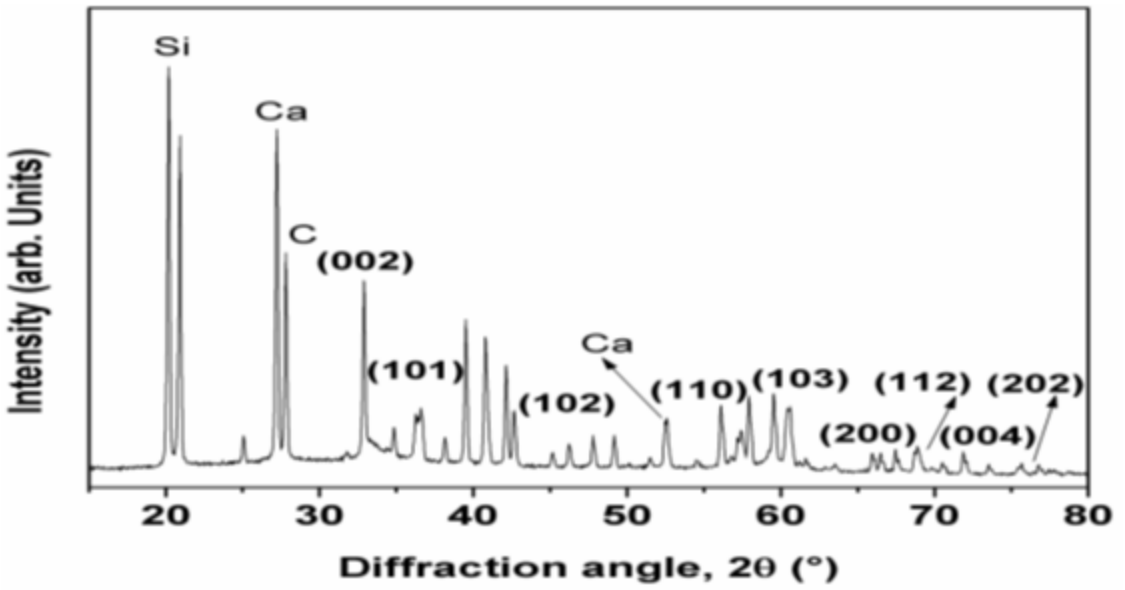

Figure 5

X-ray diffraction micrograph of biosynthesized *Ae*-ZnONPs representing the wurtzite's hexagonal structure

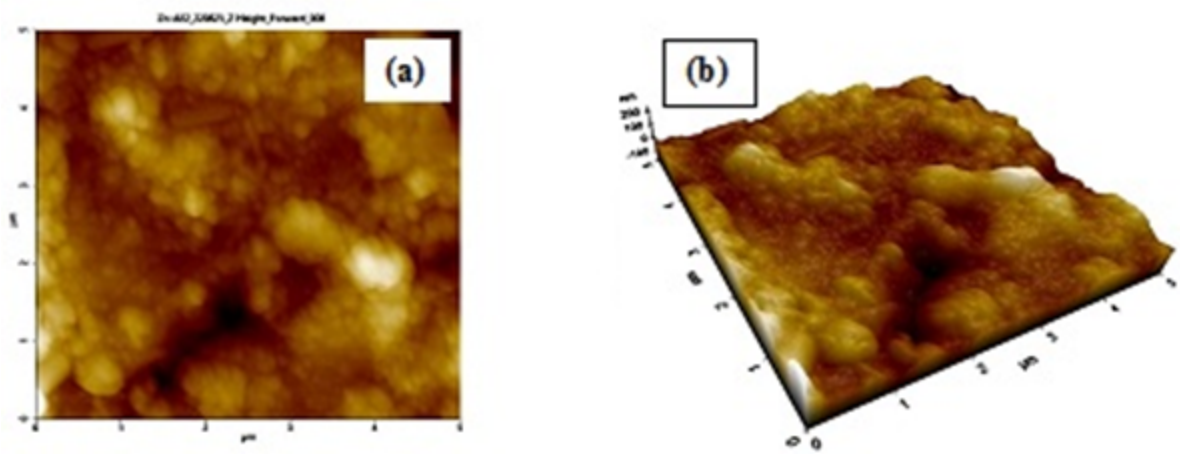

Figure 6

Surface topography of Synthesized *Ae*-ZnONPs

(a) 5 µm resolution **(b)** 3dimensional view of *Ae*-ZnONPs

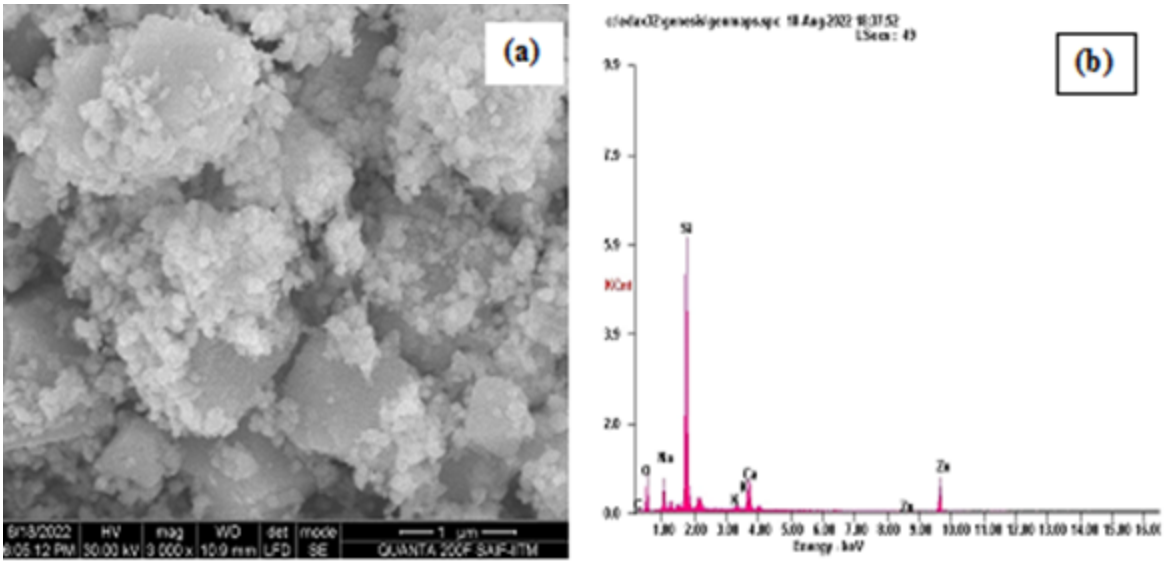

Figure 7

(a) Micro Structural images of *Ae*-ZnONPs

(b) EDX analysis of synthesized *Ae*-ZnONPs

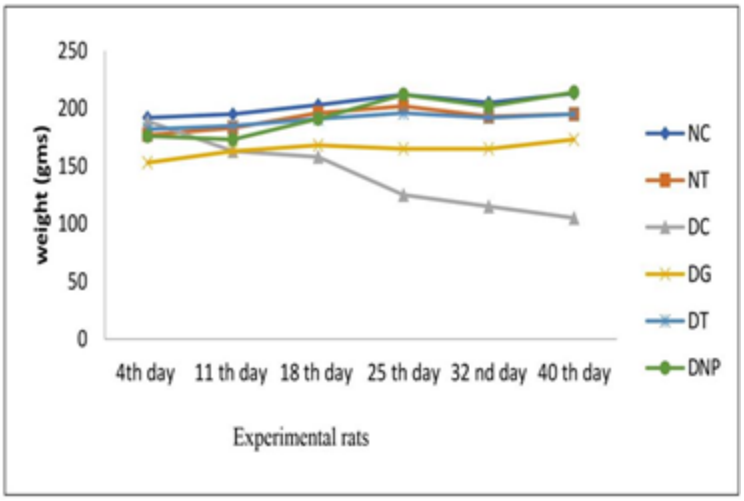

Figure 8

Effect of AeEE, *Ae*-ZnONPs on body weight of normal and experimental diabetic rats.

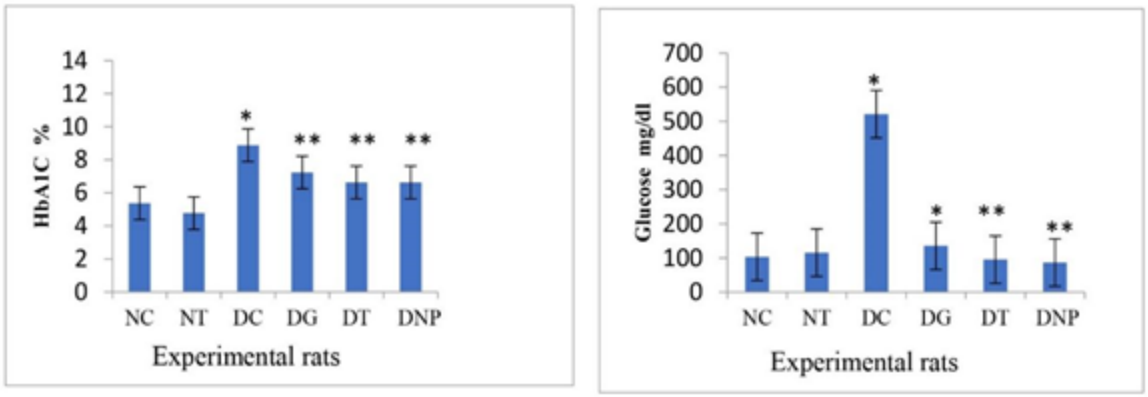

Figure 9

Impact of AeEE, *Ae*-ZnONPs on HbA_1c, Fasting blood glucose (FBG) values in normal and diabetic rats treated with Glibenclamide, AeEE and *Ae*-ZnONPs. Results are presented as mean ±S.D. of six rats from each group. Statistical significance (*P<0.05, **P<0.01)

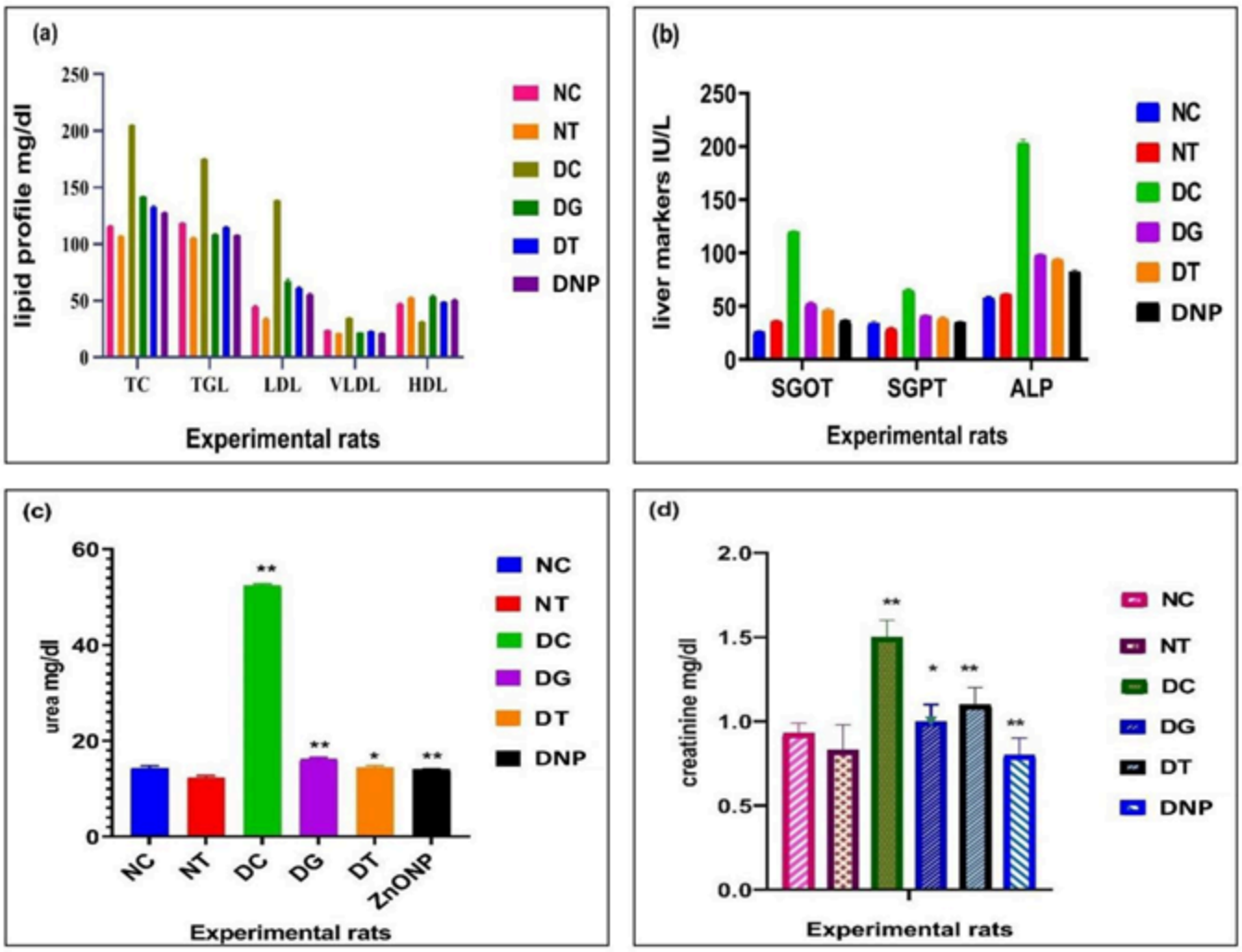

Figure 10

Effect of *Ae*-ZnONPs on STZ-induced diabetic rats **(a)** serum lipid profile (total cholesterol, triglycerides, LDL, VLDL, HDL) **(b)** liver marker enzymes (SGOT, SGPT, ALP) **(c)** urea and **(d)** creatinine in normal and diabetic rats after long term treatment. Results are presented as mean ±S.D. (n=6) and Statistical significance (*P<0.05, **P<0.01)

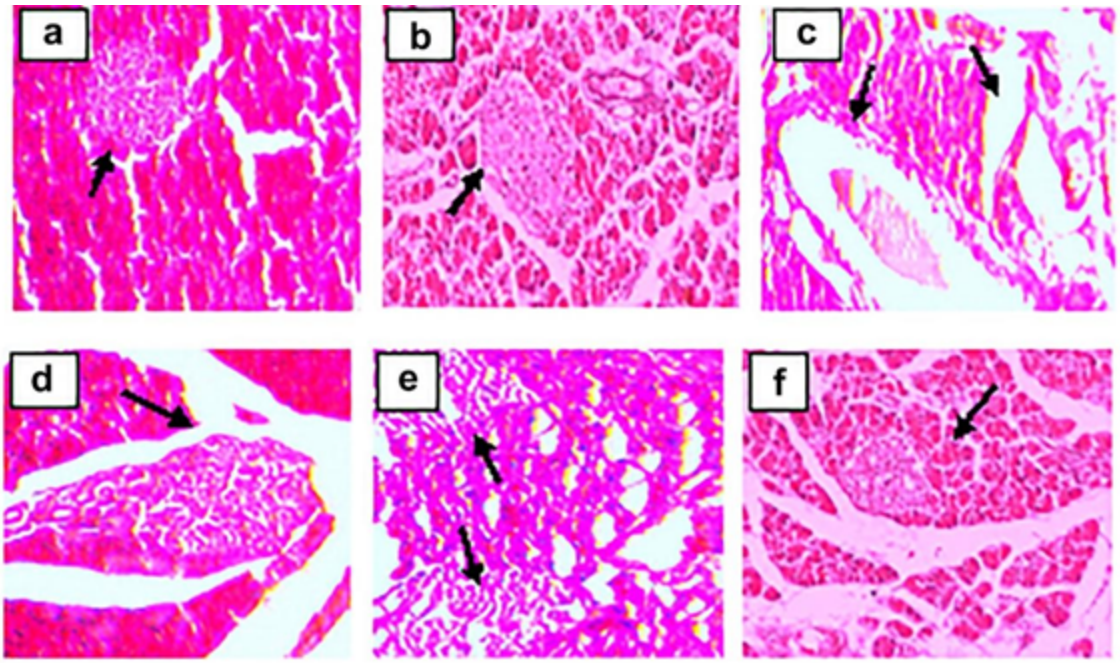

Figure 11

Photomicrograph of pancreatic tissues of experimental rats **(a)** Normal control rats showing normal islet of Langerhans in between normal pancreatic acini and pancreatic duct **(b)** Normal treated rats shows normal cell architecture **(c)** Diabetic control rats showing ruptured and destructed islet of Langerhans with damage in β cells **(d)** Diabetic Glibenclamide rats shows normal islets of Langerhans with congestion in islets capillaries **(e)**Diabetic rats treated with AeEE shows apparently normal islet of Langerhans with low density **(f)** Nanoparticle treated rats shows normal cells with more number of β cells